Asian Journal of Chemistry; Vol. 29, No. 10 (2017), 2154-2158

ASIAN JOURNAL OF CHEMISTRY

https://doi.org/10.14233/ajchem.2017.20669

# Copper Metallic Powder Effect for Expanded Graphite Plate for Thermal Conductivity

DINH CUNG TIEN NGUYEN, BISWAS MD ROKON DOWLA, YONRAPACH AREEROB, ASGHAR ALI and WON-CHUN OH*

Department of Advanced Materials Science & Engineering, Hanseo University, Seosan-si, Chungnam 356-706, Republic of Korea

*Corresponding author: Fax: +82 41 6883352; Tel: +82 41 6601337; E-mail : wc_oh@hanseo.ac.kr

*Received*: 25 March 2017; *Accepted*: 15 June 2017; *Published online*: 31 August 2017; AJC-18510

In this study, the copper metallic powder effect for expanded graphite plate was considered to thermal conductivity. The samples were evaluated by various techniques such as scanning electron microscopy (SEM), wear rate, compressive strength, shore hardness, thermal conductivity and heat conduction. The achieved results expected not only to expand the applications of carbon materials but also to popularize new concept concrete flooring and concrete interior products that can maximize energy efficiency using low power as well as the new industry to respond to future changes in the investment policies around the world to take advantage of the expanded graphite material.

**Keywords: Thermal conductivity, Expanded graphite, Artificial marble, Concrete flooring.**

## INTRODUCTION

Due to its more styles, easily processing, beautiful, rich colours and aesthetic qualities, marble is known as the high-class product, which is used for a variety purposes such as flooring, furniture, walling and *etc*. It includes natural marble and artificial marble (engineered stone) [1-4]. Nowadays, in the market, natural marble flooring with the total thickness about 12-20 mm is evaluated too expensive, low intensity, increased heating costs, slippery and maintenance difficulty. Therefore, marble composite plate structure and artificial marble (engineered stone) as products are shown in Fig. 1 have been presented to overcome above disadvantages. In order to solve these problems, we have been developing new materials and manufacturing techniques for concrete kitchen tops that can complement the disadvantages (weak strength, high prices, *etc*.) of natural marble and artificial marble (engineered stone). It will become the possibility of pioneering a new trend of kitchen top market and concrete interior field with various functions and advantages.

In order to enter the interior of concrete products market, the usability, durability, economy and aesthetics must be evaluated excellently compared to conventional interior products. On the other hand, the development of technology and material must be considered. At present, the various materials such as fiber, polymer, functional aggregate and loss are applied to each property to make concrete functional [5-11]. Recently, nanocarbon materials are evaluated as a core material of 21st century with excellent characteristics which are used in various fields such as displays, ultra light/high strength materials and printing electronic materials [12-14]. In the concrete field, graphite and carbon materials are used for reinforcing concrete, electrical conductive concrete and concrete pavement [15]. In spite of the outstanding characteristics of materials, carbon materials have limitations in growing into secondary products due to high prices. It is necessary to develop application products using low-quality carbon materials overcome that problem. This study can be expected not only to expand the applications of carbon materials but also to popularize new concept concrete flooring and concrete interior products that can maximize energy efficiency using low power.

## EXPERIMENTAL

Exfoliated-graphite was prepared in the laboratory from natural graphite and was used in the formation of samples. Sand was collected in university campus. Copper (Cu, powder 150-300 mesh, 99.5 %) was purchased from Samchun Pure Chemicals Co. Ltd., Korea. Phenolic resin was purchased from Kangnam Chemical Co., Ltd, Korea. Sulfuric acid ($H_2SO_4$, 98 %) was purchased from Daejung Chemicals Co. Ltd., Korea. Ethanol ($C_2H_5OH$, 95 %) was purchased from Duskan Pure Chemicals Co. Ltd., Korea. All the chemicals were used without further purification.

**Preparation of sand powder:** Sand collected was then washed away from muds and dust. After drying under vacuum, the dried sand was ground with ball mill grinder machine to make sand powder. A moderate amount of dried sand are placed into the mill drum and rotated with the ball that is to be crushed. The achieved sand powder was smoothed by sieve.


Fig. 1. Marble flooring products of (a) natural marble composite tiles (b) artificial marble flooring

**Preparation of graphite sheet:** The graphite intercalation compounds (GICs): $H_2SO_4$-GICs was synthesized in the laboratory from natural graphite [16]. The product was washed with distilled water 3 times. After drying under vacuum at 105 °C for 24 h, the achieved compounds were dried at room temperature to 500 °C for 8 h followed by heating at 500-600 °C for 1 h. The SEM image of exfoliated graphite was presented in Fig. 2.

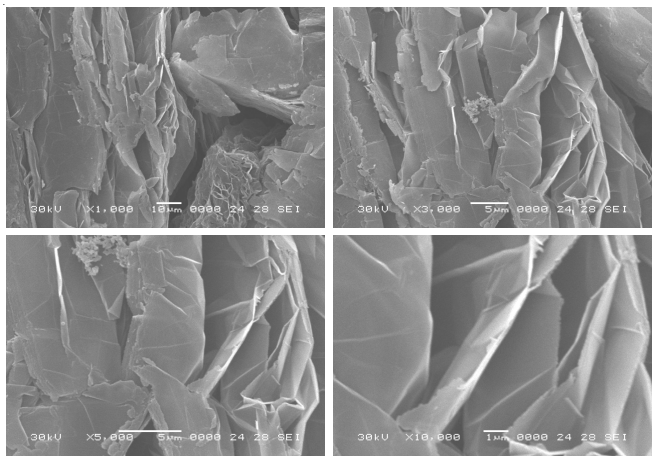

Fig. 2. SEM pictures after expansion

**Preparation of SC:** In a typical procedure for preparing SC, a certain amount of sand powder, ex-graphite and phenolic resin was mixed together. The mixture was smoothed by sieve. After that, a certain amount of Cu was added to a smoothed powder to form the final mixture for preparing SC. The samples were labeled as SC1, SC2 and SC3 corresponding to different amounts of sand, ex-graphite, phenolic resin and Cu as shown in Table-1. Finally, the above powder was mixed with 10 mL ethanol and put in the mold, press by hydrologic pressure to form SC1, SC2 and SC3 blocks.

TABLE 1
COMPOSITION AND CONTENT OF THERMOREGULATED DECORATING FLOORING, WHICH IS A FUSION OF EXPANDED GRAPHITE WITH THERMAL CONDUCTIVITY AND CONCRETE

| Ingredient | Sand (wt %) | Exfoliated graphite (wt %) | Metal (wt %) | Phenolic resin (wt %) | Metal |
|---|---|---|---|---|---|
| SC1 | 58.8 | 23.5 | 2.91 | 14.7 | Cu |
| SC2 | 57.1 | 22.9 | 2.82 | 17.1 | Cu |
| SC3 | 55.6 | 22.2 | 2.77 | 19.4 | Cu |

**Characterization:** The shape and structure of the nano-material surface with high resolution are analyzed using the SEM method (JSM-5600 JEOL, Japan).

The wear rate was calculated using the following expression as:

$$\text{Wear rate (\%)} = \frac{\text{Weight before test (g)} - \text{Weight after test (g)}}{\text{Weight before test (g)}} \times 100$$

The compressive strength of the material divided into fragments can be defined in a narrow sense as an independent property. In compressive tests, the compressive strength is calculated by dividing the maximum load by the initial cross-sectional area of the specimen. The compressive strength was calculated as Fig. 3 an the following expression:

$$\sigma_{fs} = \sigma_m^{fail} = \frac{1.5F_{max}L}{bd^2} = \frac{F_{max}L}{\pi R^3}$$

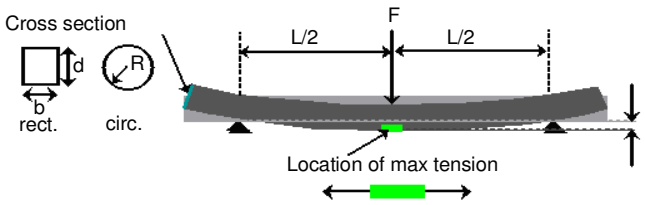


Fig. 3. Compressive strength measurement

Electrical conductivity is a unit that indicates the ability of a single material to conduct current, whereas a non-electrical conductivity is a unit of electrical conductivity of an object having a unit of length or unit of an area under a specific temperature. The unit of electrical conductivity is mho or siemens and 1 mho = 1 siemen. Electrical conductivity refers to the extent to which a substance or solution to carry current. It can be evaluated expressed as the reciprocal of the electrical resistance ($\Omega^{-1}$) or voltage S (siemens) to the solution.

The resistance R in which the conductors are as follows $R = \rho * I/S$ where $\rho$ is the resistivity ($\Omega$ m), I is the distance between the two electrodes (m) and S is the cross-sectional area ($m^2$). Therefore, the electrical conductivity L was calculated as $L = 1/R = S/(\rho I)$.

The shore hardness test shows a hardness value based on the rebound height of a hammer falling vertically on a piece of test at a fixed height. The shore hardness is measured by a small hammer (diameter: 1/4", length: 3/4") attached to the bottom of a steel bar with a diameter of 0.02 in diameter

(diamond blur) which was placed in a 10"- height glass tube. The hardness is adjusted by reading the scale attached to the inner wall of the pipe at the maximum height at which the upper end of the hammer reaches, when it falls on the surface of the specimen and protrudes by elasticity. The shore hardness value is $H_s$.

Shore hardness of sample was calculated using the following expression $H_s = (kh)/h_0$, where $H_s$ is shore hardness value, k is constant for determining shore hardness, h is drop height and $h_0$ is height of repulsion.

The thermal conductivity of sample was calculated using the following expression, $\lambda = \alpha\rho C_p$, where $\alpha$ is the thermal diffusivity, $\rho$ is the bulk density and $C_p$ is the specific heat.

Heat conduction test is a general method of heat flow method. It can be expressed as Fourier's law in the case of a steady state measured at a constant temperature distribution.

$$q/A = -k*dT/dx$$

where q is calorie, A is area, k is thermal conductivity, dT is temperature difference and dx is Fourier's law of distance is not an induction from an equation but an empirical formula.

## RESULTS AND DISCUSSION

Morphology of the exfoliated graphite was characterized for the initial evaluation by SEM methods and the results were presented in Fig. 2. The results in Fig. 2 show that the GICs exhibited a much rougher basal plane with sharp and delaminated edges after intercalation as well as the separation sign between graphene layers along the edge.

Wear test was carried out to predict the wear performance and the results were presented in Table-2. The wear rates are calculated results reflecting wear mass loss. As the result, the survey samples were shown the low abrasion rate around 0.144-0.949 %. It was observed that the mass of material lost due to wear is relatively small. The above results indicated the relatively durable state of survey samples according to the test condition.

TABLE-2
RESULTS OF WEAR RATE MEASUREMENT

| Sample name | Run | Wear amount (mg) | Abrasion rate (%) |
|---|---|---|---|
| SC1 | 1 | 11 | 0.043 |
| | 2 | 92 | 0.377 |
| | 3 | 3 | 0.012 |
| | Average | 35 | 0.144 |
| SC2 | 1 | 110 | 0.468 |
| | 2 | 181 | 0.726 |
| | 3 | 538 | 1.654 |
| | Average | 276 | 0.949 |
| SC3 | 1 | 61 | 0.241 |
| | 2 | 3 | 0.012 |
| | 3 | 53 | 0.214 |
| | Average | 39 | 0.156 |

The compression strength information was presented in Fig. 4. Under the maximum pressure, the material can be subjected to compressive loading, the compression of the material is divided into fragments that can be defined in a narrow sense as an independent property. However, the

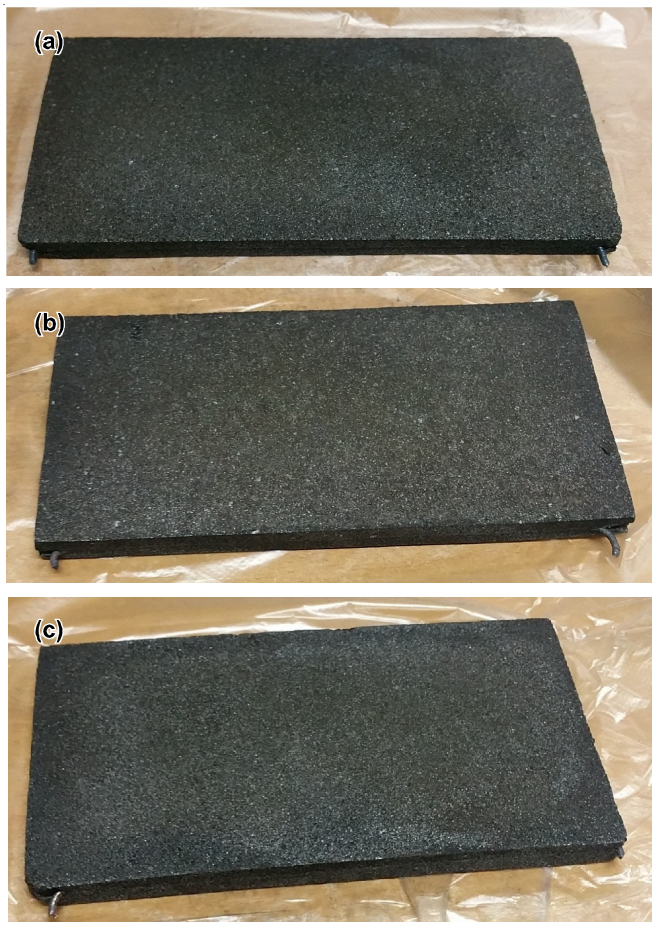


Fig. 4. Samples for physical property evaluation (a) SC1, (b) SC2, and (c) SC3 samples

compressive strength of the uncompressed material must be determined as the amount of pressure required to distort any amount of material. The compressive strength in the compression test is calculated by giving the maximum load divided by the area of the initial cross-section of the sample. The compressive strength according to the presence of binder was measured and the results were summarized in Table-3. It showed different intensity values of 2-3 times corresponding to the before and after the heat treatment process. As a result, the value of strength value decreases as binder content increases. This result indicates that sand is the main material of concrete, which has a great effect on the strength value. The addition of metallic copper is promised as a valuable lead to a relatively high power.

TABLE-3
COMPRESSION STRENGTH OF SC1, SC2, AND SC3 SAMPLES

| Sample name | Before heat treatment | After heat treatment |
|---|---|---|
| SC1 | 31 | 11 |
| SC2 | 29 | 9 |
| SC3 | 24 | 4 |

The shore hardness was measured in terms of the binder content and the results were summarized in Table-4. From Table-4, we can see much difference before and after heat treatment process. The result shows that the heat treatment has a considerable influence on hardness. According to the results, the hardness value showed a tendency to increase as

TABLE 4
SHORE HARDNESS OF SC1, SC2, AND SC3 SAMPLES

| Sample name | Before heat treatment | After heat treatment |
|---|---|---|
| SC1 | 20 | 9 |
| SC2 | 26 | 6 |
| SC3 | 23 | 11 |

the binder content increased. On the other hand, the content of sand and binder, which is the main material of concrete has a great influence on the hardness value.

The electrical resistivities were measured and the results were summarized in Table-5. As expected, it showed many differences corresponding to the before and after the heat treatment process. The thermal resistivity has a considerable influence on the electrical resistivity. It is determined that the variable heat treatment had a great effect on the alignment of the carbide and the organizational structure of the binder. Besides, as the amount of binder increased, the electrical resistivity value showed a tendency to decrease. In Table-5, the presence of sand and binder, which is the main material of concrete has a great influence on the electrical resistivity value. Moreover, the addition of copper as the metal components exhibited a relatively high electrical resistivity. The copper component has exhibited the effect of lowering the electrical resistivity significantly.

TABLE-5
ELECTRICAL CONDUCTIVITY OF
SC1, SC2, AND SC3 SAMPLES

| Sample name | Before heat treatment ($\times 10^{-3}$, Ω cm) | After heat treatment ($\times 10^{-3}$, Ω cm) |
|---|---|---|
| SC1 | 8.25 | 24.5 |
| SC2 | 6.34 | 18.5 |
| SC3 | 6.23 | 14.3 |

The thermal conductivity results after heat treatment process are shown in Fig. 5. As a result, the value of thermal conductivity is significantly influenced by the reduced amount of sand and metal as well as the increased the binder amount. It is judged that the metal component and the binder primarily affect the carbonization and the texture structure orientation. Moreover, the high resistance of sand has a considerable influence on the thermal conductivity. As the content of binder increased, the thermal conductivity value showed a tendency to increase. It can be seen that the presence of sand and binder which is the main material of concrete has a significant influence on the thermal conductivity value. On the other aspects, the addition of copper as a metal (sample SC3) showed relatively high thermal conductivity values. This shows that the effect of increasing the thermal conductivity value of metal component is also remarkable.

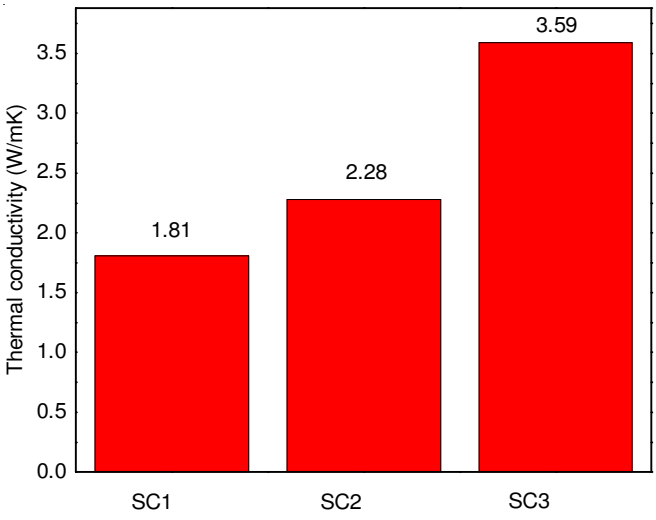


Fig. 5. Thermal conductivity value of SC1, SC2 and SC3 samples

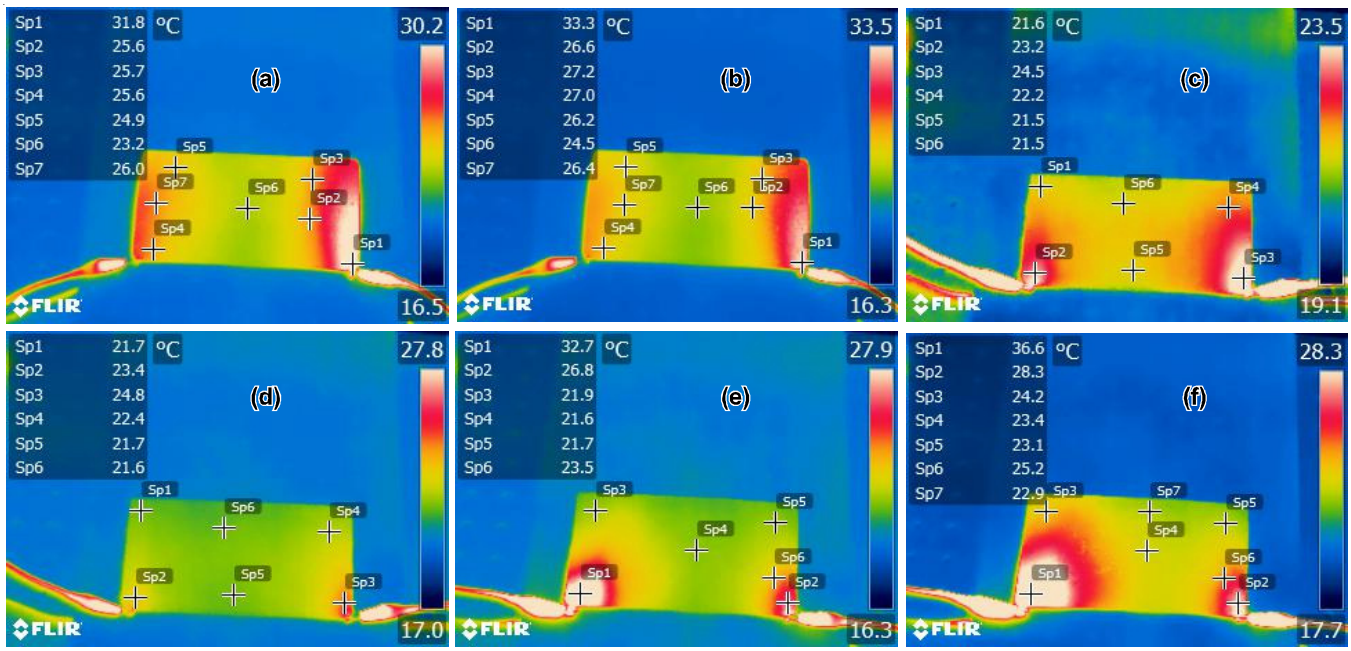


Fig. 6. Thermal image of different kind of (a) SC1: Applied current 4Amp for 3 min, (b) SC1: Applied current 4 Amp for 5 min, (c) SC2 : Applied current 4 Amp for 3 min, (d) SC2 : Applied current 4Amp for 5 min, (e) SC3 : Applied current 4Amp for 3 min and (f) SC3: Applied current 4 Amp for 5 min

The relationship between the time, electric conductivity and thermal conductivity value of SC1, SC2 and SC3 samples was measured by using a thermal camera. After annealing, the results of these correlations are shown in Fig. 6. The results showed that the electric conductivity and thermal conductivity have a considerable influence on the relationship between the decreased of sand and metal amount, as well as the increased of binder amount. This indicates that the metal components and the binder mainly affect the carbonization and the orientation of the structure. Besides, these factors have a great influence on the relationship between time, electric conductivity and thermal conductivity.

Through the results in Fig. 6 and above results, it is concluded that the high resistance of sand is a factor that has a considerable influence on the thermal conductivity. The thermal distribution also increased with increasing binder content. With the presence of copper as a metal component, SC1 is shown a shape of relatively uniform thermal distribution more than that on SC2 and SC3 samples. This has been significantly effective metal components to increase the distribution of heat in the present development.

## Conclusion

New markets can be created by expanded graphite, which can be mass-produced at low cost. Engineered stone, one of the artificial marbles developed to overcome the performance limitations, is expensive and not widely used. The combination and ratio of concrete and carbon material constituting material are possible to increase energy efficiency by developing the composite material that shows various physical properties such as electromagnetic wave shielding and heat generation.

## ACKNOWLEDGEMENTS

This work (Grants No. C0397478) was supported by Business for Cooperative R&D between Industry, Academy and Research Institute funded Korea Small and Medium Business Administration in 2016.

## REFERENCES

1. T.B. Afeni and S.K. Osasan, *Mining Sci. Technol. (China)*, **19**, 420 (2009); https://doi.org/10.1016/S1674-5264(09)60078-8.
2. N. Careddu and G. Siotto, *Resour. Policy*, **36**, 304 (2011); https://doi.org/10.1016/j.resourpol.2011.07.002.
3. J.T. Alvarez, I.D. Alvarez and S.T. Lougedo, *WIT Transac. Ecol. Environ.*, **116**, 85 (2008); https://doi.org/10.2495/AIR080101.
4. E.C. Cromley, *Mater. History Rev.*, **44**, 8 (1996).
5. C. Meyer, S. Baxter and W. Jin, Alkali-Aggregate Reaction in Concrete with Waste Glass as Aggregate, In: Proceedings of 4th Materials Engineering Conference: Materials For The New Millennium. Reston, VA, pp. 1388–1397 (1996).
6. C. Meyer and S. Baxter, Use of Recycled Glass and Fly Ash for Precast Concrete, Rep. NYSERDA 98-18 (4292-IABR-IA-96) to New York State Energy Research and Development Authority, Columbia University, New York, USA (1998).
7. C. Polley, S.M. Cramer and R.V. Cruz, *J. Mater. Civ. Eng.*, **10**, 210 (1998); https://doi.org/10.1061/(ASCE)0899-1561(1998)10:4(210).
8. Z.P. Bazant, G. Zi and C. Meyer, *J. Eng. Mech.*, **126**, 226 (2000); https://doi.org/10.1061/(ASCE)0733-9399(2000)126:3(226).
9. E.A. Byars, B. Morales-Hernandez and H.Y. Zhu, *Concrete*, **38**, 41 (2004).
10. I.B. Topcu and M. Canbaz, *Cement Concr. Res.*, **34**, 267 (2004); https://doi.org/10.1016/j.cemconres.2003.07.003.
11. C.H. Chen, R. Huang, J.K. Wu and C.C. Yang, *Cement Concr. Res.*, **36**, 449 (2006); https://doi.org/10.1016/j.cemconres.2005.12.010.
12. S.V. Morozov, K.S. Novoselov, M.I. Katsnelson, F. Schedin, D.C. Elias, J.A. Jaszczak and A.K. Geim, *Phys. Rev. Lett.*, **100**, 016602 (2008); https://doi.org/10.1103/PhysRevLett.100.016602.
13. Z.S. Wu, G.M. Zhou, L.C. Yin, W.C. Ren, F. Li and H.M. Cheng, *Nano Energy*, **1**, 107 (2012); https://doi.org/10.1016/j.nanoen.2011.11.001.
14. S. Bae, H. Kim, Y. Lee, X.F. Xu, J.S. Park, Y. Zheng, J. Balakrishnan, T. Lei, H.R. Ri Kim, Y. Song, Y.-J. Kim, K.S. Kim, B. Özyilmaz, J.-H. Ahn, B.H. Hong and S. Iijima, *Nat. Nanotechnol.*, **5**, 574 (2010); https://doi.org/10.1038/nnano.2010.132.
15. S. Wu, X. Liu, Q. Ye and N. Li, *Trans. Nonferr. Met. Soc. China*, **16**, 512 (2006); https://doi.org/10.1016/S1003-6326(06)60246-X.
16. Y. Geng, Q. Zheng and J.-K. Kim, *J. Nanosci. Nanotechnol.*, **11**, 1084 (2011); https://doi.org/10.1166/jnn.2011.3063.